

# The Structural Basis for Metal Ion Transport in the SLC11/NRAMP Family

Cristina Manatschal and Raimund Dutzler\*

**Abstract:** The SLC11/NRAMP proteins constitute a conserved family of metal ion transporters that are expressed in all kingdoms of life. In humans, the two paralogs DMT1 and NRMP1 play an important role in iron homeostasis and the defense against pathogens. SLC11 transporters have evolved an exquisite selectivity for transition metal ions, which facilitates their efficient transport from a large background of  $\text{Ca}^{2+}$  and  $\text{Mg}^{2+}$ . This is accomplished by the evolution of a conserved binding site, which contains besides promiscuous hard ligands, a methionine acting as soft ligand that exclusively coordinates transition metals and thus contributes to the exclusion of alkaline earth metal ions. This site is altered in a branch of prokaryotic family members, which are capable of transporting  $\text{Mg}^{2+}$ , where the removal of the coordinating methionine and the accompanying expansion of the binding pocket captures this small ion in a hydrated state. The disposition of titratable residues in  $\text{H}^+$ -coupled transition metal ion transporters, that are absent in uncoupled  $\text{Mg}^{2+}$  transporters, sheds light on potential coupling mechanisms. In combination, the discussed work has revealed detailed insight into transition metal ion transport and provides a basis for the development of inhibitors of DMT1 as strategy against iron overload disorders.

**Keywords:** DMT1 · Secondary active transport · Transition metal ion selectivity



**Raimund Dutzler** studied Biochemistry at the University of Vienna and worked with Prof. Tilman Schirmer at the Biozentrum of the University of Basel during his PhD studies. He joined the group of Prof. Roderick MacKinnon at the Rockefeller University for his PostDoc. In 2003, he was appointed as Assistant Professor at the Department of Biochemistry of the University of Zurich and was promoted to

the rank of Full Professor in 2009. Work in the Dutzler group focuses on the mechanisms of ion and lipid transport. In the framework of the NCCR TransCure, the group has investigated iron transporter families.



**Cristina Manatschal** studied Biochemistry at ETH Zurich and carried out her PhD studies in the group of Dr. Michel Steinmetz at the Paul Scherrer Institute. For her PostDoc, she joined the group of Prof. Raimund Dutzler at the Department of Biochemistry of the University of Zurich, where she has characterized iron transporters of the SLC11 and SLC40 families by X-ray crystallography, cryo-electron

microscopy and biochemical assays. Since 2022, she is Lecturer and Teaching Coordinator at the Department of Biochemistry of the University of Zurich.

## 1. Divalent Cations in Biology

Divalent metal ions play important roles throughout biology, and they constitute a major fraction of the mineral content of our body. The two most abundant ions in this respect derive from the alkaline earth metals calcium and magnesium, both residing in the

same group of the periodic system. Owing to their high net charge, both ions strongly interact with either inorganic or organic anions. This property facilitates the formation of stable macroscopic structures, such as bone, and the interaction with anionic groups in proteins and nucleic acids to contribute to diverse cellular processes. The latter is exemplified by the role of  $\text{Ca}^{2+}$  in signaling, muscle contraction and the activation of enzymes<sup>[1]</sup> and the role of  $\text{Mg}^{2+}$  in masking the phosphate groups of nucleotides and nucleic acids.<sup>[2]</sup> The distinct chemical features of both ions originate from differences in their ionic radius and the consequent altered surface charge density. The smaller  $\text{Mg}^{2+}$  shows increased affinity to water, rendering its dehydration energetically costly, which is reflected in the construction of its molecular interaction sites.<sup>[3]</sup> Besides  $\text{Ca}^{2+}$  and  $\text{Mg}^{2+}$ , our body also requires other divalent cations that are part of the region in the periodic system encompassing transition metals. Transition metal ions of biological relevance, which include  $\text{Fe}^{2+}$ ,  $\text{Cu}^{2+}$ ,  $\text{Zn}^{2+}$ ,  $\text{Mn}^{2+}$  and  $\text{Co}^{2+}$ , share chemical properties that are not accounted for by a classical description of ions as charged spheres.<sup>[4,5]</sup> They are distinguished by their incompletely filled d-orbitals, which allows them to undergo coordinative interactions with free electron pairs of atoms. This property is reflected in transition metal ion binding sites, which frequently contain sulfur and nitrogen as ligands,<sup>[6,7]</sup> and it enables  $\text{Fe}^{2+}$  to bind the apolar oxygen in the transport proteins hemoglobin and myoglobin.<sup>[8]</sup> A second feature of certain transition metal ions concerns their ability to transit between oxidation states, which renders  $\text{Fe}^{2+}$ ,  $\text{Mn}^{2+}$  and  $\text{Cu}^{2+}$  versatile cofactors for redox reactions.<sup>[9]</sup> In all cases, the discussed ions need to be taken up by the organism and distributed to different organs, which requires their transport across cellular membranes and their concentration within cells. This process is to a large extent performed by transmembrane transport proteins. Metal ion transporters selectively capture their targets and mediate their movement across the low-dielectric environment of the cell membrane, which creates an impermeable barrier for ions. The energy required for the intracellular accumulation originates from the negative membrane potential, which itself facilitates the concentration of cations, and in certain cases by the coupling to either ATP hydrolysis or the downhill transport of another ion. In the framework of the NCCR TransCure, we became interested in

\*Correspondence: Prof. R. Dutzler, E-mail: dutzler@bioc.uzh.ch  
Dept. of Biochemistry, University of Zurich, Zurich, CH-8057 Zurich

members of the SLC11/NRAMP family, which catalyze the import of  $\text{Fe}^{2+}$  and  $\text{Mn}^{2+}$  into the cytosol, powered by the cotransport of  $\text{H}^+$  serving as energy source.<sup>[10]</sup> In this short review, we will focus on the structural basis for ion selectivity and transport in this ubiquitous protein family, whereas biological mechanisms of  $\text{Fe}^{2+}$  transport and associated diseases are covered in an accompanying article in the same issue. By summarizing recent work by us and others on the structure and function of family members, we refer to our activities performed in the context of TransCure.

## 2. The SLC11/NRAMP Family

Iron uptake in the small intestine either proceeds as free  $\text{Fe}^{2+}$  or in its complex with heme by different transport proteins located on the apical side of the duodenum.<sup>[10]</sup> Within the body, cellular iron uptake is mediated as a complex of  $\text{Fe}^{3+}$  bound to the carrier transferrin by receptor-mediated endocytosis.<sup>[11]</sup> Divalent metal ion transporter 1 (DMT1) was identified as the primary transport system for free  $\text{Fe}^{2+}$  in 1990.<sup>[12]</sup> The protein is part of the conserved solute carrier 11 (SLC11) family that is expressed in all kingdoms of life.<sup>[13]</sup> In mammals, this family contains a second paralog named natural resistance-associated macrophage protein 1 (NRAMP1, SLC11A1)<sup>[14]</sup> that was identified to contribute to the cellular defense against infections with mutations contributing to bacterial resistance. Whereas expression of DMT1 (SLC11A2) is ubiquitous, NRAMP1 is confined to macrophages. In most cells, both SLC11 family members transport endocytosed iron from intracellular organelles into the cytoplasm.<sup>[10]</sup> This process is powered by the  $\text{H}^+$  gradient generated by the vesicular ATPase, which also catalyzes the acidification of the vesicle causing the release of the metal ion from transferrin. Additionally, DMT1 is expressed on the apical side of the plasma membrane of enterocytes where it directly mediates the cellular import of  $\text{Fe}^{2+}$  from the intestinal lumen, powered by the  $\text{H}^+$  gradient that exists between the cytoplasm and the unstirred acidic layer at the surface of the epithelium.<sup>[15]</sup> Highly homologous SLC11 proteins are also found in bacteria, where they are responsible for the uptake of  $\text{Mn}^{2+}$  since, in prokaryotes, iron is usually transported as complex to siderophores by unrelated transporter families.<sup>[16,17]</sup> Similarly, SLC11 family members in plants are responsible for the uptake of desired trace metals but also for the detoxification of metals such as  $\text{Cd}^{2+}$ .<sup>[18]</sup>

## 3. Functional Properties of SLC11 Transporters

On a functional level, the best characterized family member is the human transporter DMT1, which was studied following its overexpression in *X. laevis* oocytes by electrophysiology and radioactive transport assays.<sup>[12,19]</sup> These experiments demonstrated the electrogenic symport of different transition metals coupled to the cotransport of  $\text{H}^+$ , although the coupling was described as comparatively weak resulting in accompanying uncoupled transport of either substrate.<sup>[20]</sup> Among divalent transition metal ions, the characterized substrate selectivity is comparably broad ranging from  $\text{Fe}^{2+}$  to  $\text{Co}^{2+}$  and  $\text{Mn}^{2+}$ .<sup>[19,21]</sup> The transport of  $\text{Cd}^{2+}$  and  $\text{Ni}^{2+}$  emphasizes the role of the protein in the undesired uptake of toxic metal ions. Despite the poor discrimination between transition metals,  $\text{Ca}^{2+}$  and  $\text{Mg}^{2+}$  are not transported substrates, although one study suggests a weak inhibition of metal ion transport by  $\text{Ca}^{2+}$  at high mM concentrations.<sup>[22]</sup> This strong discrimination is essential to accomplish the transport of traces of transition metal ions from a large background of alkaline earth metal ions, which are several orders of magnitude more abundant. A generally similar behavior was also found in prokaryotic family members where transport was either investigated in cellular uptake studies in case of the *Escherichia coli* homologue MntH,<sup>[16]</sup> or *in vitro* for the transporters from the bacteria *Staphylococcus capitis* (ScaDMT),<sup>[23]</sup> *Deinococcus radiodurans* (DraNRAMP)<sup>[24]</sup> and *Eremococcus coleocola* (EcoDMT)<sup>[25]</sup> following the reconstitu-

tion of purified transporters into proteoliposomes. As for DMT1, transport of different divalent transition metal ions in prokaryotic homologues proceeded with  $\mu\text{M}$   $K_m$  while  $\text{Ca}^{2+}$  and  $\text{Mg}^{2+}$  were excluded.<sup>[26]</sup> In such *in vitro* studies, also the coupled cotransport of transition metal ions and  $\text{H}^+$  was demonstrated.<sup>[25]</sup> The three prokaryotic homologs ScaDMT, DraNRAMP and EcoDMT used for the investigation of ion transport *in vitro* also served as systems for structure determination.<sup>[27]</sup>

## 4. Structural Properties of SLC11 Transporters

The initial breakthrough in the structural characterization of the SLC11/NRAMP family was reached in 2014 with the elucidation of the ScaDMT structure,<sup>[23]</sup> followed by several studies on the proteins DraNRAMP<sup>[28,29]</sup> and EcoDMT.<sup>[25]</sup> These structures were all determined by X-ray crystallography, in several cases as complex with specific immunoglobulin-derived binders, which acted as crystallization chaperones to improve crystal packing. In its general organization, the family shares its topology with a diverse group of transport proteins that lack an obvious mutual sequence relationship (Fig. 1a). This topology was initially identified for the prokaryotic amino acid transporter LeuT<sup>[30]</sup> and later found in transport proteins for neurotransmitters,<sup>[31]</sup> glucose,<sup>[32]</sup> osmolytes,<sup>[33]</sup> and ions.<sup>[34]</sup> The LeuT-fold is distinguished by a modular organization of pairs of structurally related elements, that are oriented in the membrane with opposite orientation. In this organization, the first transmembrane segment of each five-helix repeat (*i.e.*  $\alpha 1$  and  $\alpha 6$ ) is unwound in its center, with residues in this region constituting the substrate binding site (Fig. 1a). Besides the described units, SLC11 transporters contain either one or two additional transmembrane helices at the C-terminus of the second repeat (Fig. 1a). These transporters operate by an alternate access mechanism, where the protein sequentially adopts conformations in which the substrate binding site located in the center of the transporter is alternately exposed to either side of the membrane *via* a spacious aqueous cavity, whereas the access from the opposite side is closed<sup>[35]</sup> (Fig. 1b). Both extreme states on the transport cycle are connected by intermediate occluded conformations, where both aqueous cavities are sealed, and the substrate is tightly coordinated by the protein. By the successive occupation of the described conformations, the substrates (*i.e.*, divalent transition metal ions and  $\text{H}^+$  in the case of SLC11 transporters) access the transporter from one side of the membrane and are released on the opposite side, leading to a net transport that is powered by the electrochemical gradients of the transported cargos. In case of symport, the transporter either cycles in a fully substrate loaded or in an unloaded state, whereas the conformational change in partly loaded transporters is energetically unfavorable. However, due to the weak substrate coupling observed for DMT1, the transition of a partly loaded transporter is probably still possible.<sup>[20]</sup> Available structures of SLC11 transporters cover most of the transport cycle including outward-facing,<sup>[25,36]</sup> occluded<sup>[36]</sup> and inward-facing states<sup>[23,28]</sup> in absence and presence of bound substrates, which together provide a glimpse on the accessible conformational changes (Fig. 1c,d). During transport,  $\alpha$ -helices of the two subdomains move in concert, in a process that was referred to as rocking bundle mechanism.<sup>[37]</sup> In the transition from the outward- to an inward-facing conformation, a hinge-like movement of  $\alpha$ -helices 4 and 5 and a larger rearrangement of  $\alpha$ -helix 1a opens the cavity that is accessible from the cytoplasm. At the same time, the outward facing cavity is closed by smaller movements of  $\alpha$ -helices 1b, 2, 6a and 10.<sup>[25]</sup> The general conservation between the structure of prokaryotic transition metal ion transporters and human DMT1 is illustrated in their interaction with benzyl-bis-isothiourea compounds, which have been identified to inhibit both classes of transporters by occupying the cavity leading to the substrate-binding site in the outward-facing conformation of the transporter.<sup>[26]</sup>

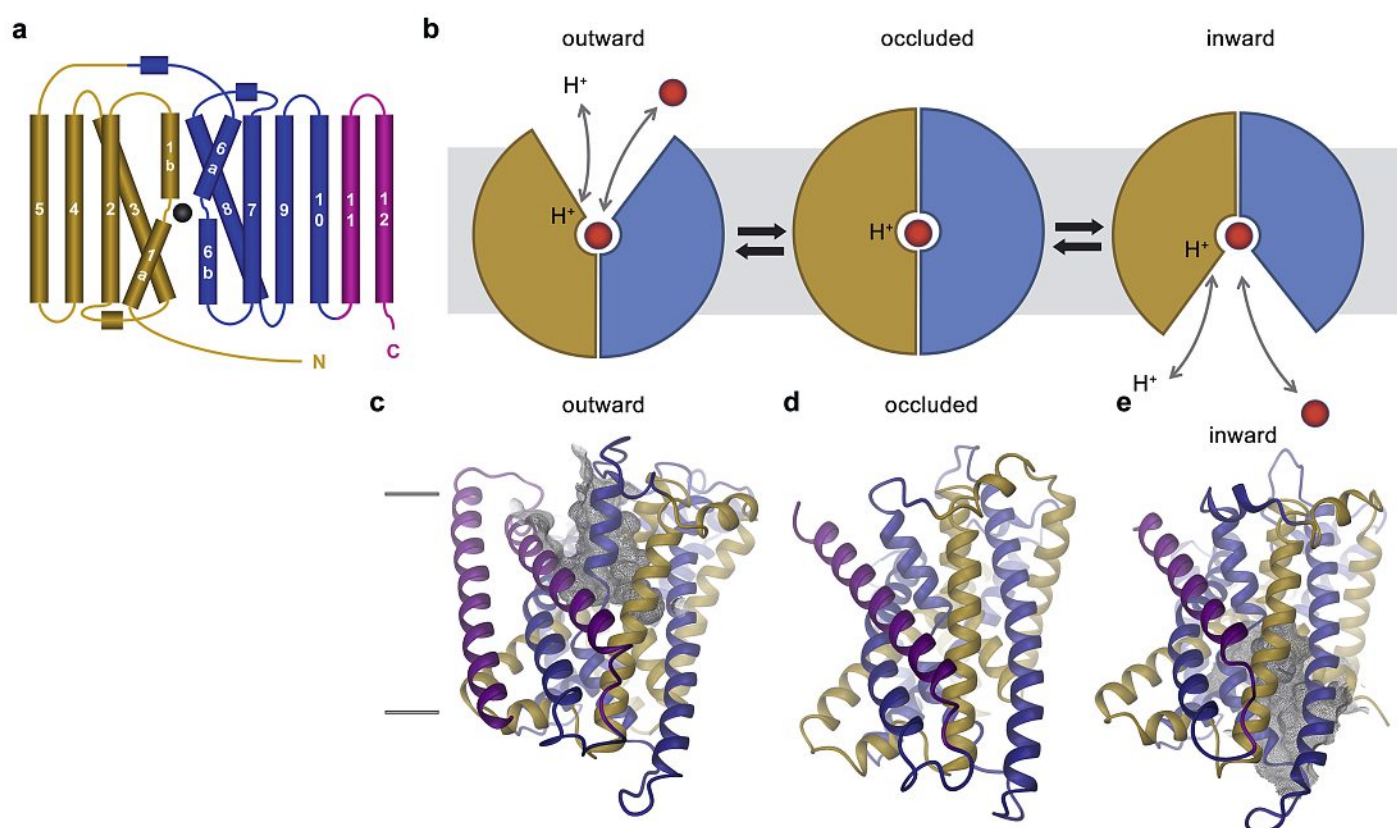


Fig. 1. SLC11 structures. a) Topology of an SLC11 transporter. The two structurally related units, consisting of five membrane spanning  $\alpha$ -helices each, are colored in orange and blue, additional helices following the second repeat in magenta. The black sphere indicates a bound transition metal ion. b) Schematic representation of major conformations on the transport cycle. c–e) Ribbon representation of prokaryotic SLC11 transporters in indicated conformations. The coloring is as in a. c) Structure of EcoDMT (PDBID 5M87) in an outward-facing conformation. d) Structure of DraNRAMP (PDBID 6C3I) in an occluded conformation. e) Structure of ScaDMT (PDBID 5M95) in an inward-facing conformation. c,e) Surface of the aqueous cavity leading to the substrate binding site is displayed as black mesh.

## 5. Transition Metal Ion Selectivity

The described structures of prokaryotic homologs have revealed the basis of the selectivity of SLC11 transporters for transition metal ions. Structural studies have benefitted from the ability to specifically detect metal ions in crystal structures, *via* their anomalous scattering properties.<sup>[23]</sup> Such experiments have aided the identification of a selective binding site located in the center of the transporter, where the bound ion is directly coordinated by the backbone and side-chains of residues that are highly conserved in family members operating as transition metal ion transporters<sup>[23]</sup> (Fig. 2a, b). In this site, the ion has lost most of its hydration shell and is instead tightly surrounded by the protein. Residues contacting the bound substrate can be divided into soft and hard ligands based on the chemistry of their interaction. Hard ligands carry negative full- or partial charges and their interaction with the bound divalent transition metal ion is dominated by electrostatics. These ligands usually contain oxygen atoms and, in case of the SLC11 transporters, include a conserved aspartate located at the unwound part of  $\alpha$ 1, an asparagine on the same helix and the free backbone carbonyl oxygen at the C-terminus of  $\alpha$ -helix 6a<sup>[23]</sup> (Fig. 2b). In the occluded conformation of DraNRAMP, an additional glutamine side-chain located on  $\alpha$ 10 has moved towards the bound ion to complete its octahedral coordination<sup>[36]</sup> (Fig. 2c). All described residues are similarly suited to interact with divalent metal ions, and they are thus not expected to be capable of distinguishing between alkaline earth metal and transition metal ions. In contrast to hard ligands, the interaction with soft ligands, which donate free electron pairs to interact with partly filled d-orbitals, is a unique property of transition metal ions that would allow for a discrimination against alkaline earth metals.<sup>[24]</sup> In case of SLC11 transporters, soft ligand-interactions are mediated by the

free electrons of the thioether of a conserved methionine residue located on the unwound part of  $\alpha$ -helix 6b, which is in direct contact with the bound ion.<sup>[23]</sup> Consequently, the transition metal ions  $\text{Mn}^{2+}$ ,  $\text{Fe}^{2+}$ ,  $\text{Co}^{2+}$ ,  $\text{Ni}^{2+}$  and  $\text{Cd}^{2+}$  were found to bind to the described site whereas  $\text{Ca}^{2+}$  does not<sup>[23]</sup> (Fig. 2d–f). The role of this residue in the selection against alkaline earth metals is further illustrated by a mutant of the methionine to alanine, which generates a transporter that is still capable of transporting transition metal ions but where  $\text{Ca}^{2+}$  has now also become a transported substrate, whereas the smaller  $\text{Mg}^{2+}$  is still excluded.<sup>[24,38]</sup>

## 6. SLC11 Transporters with Altered Selectivity

Whereas the exquisite selectivity properties for transition metals of the bulk of SLC11 transporters is reflected in the strong conservation of their metal ion binding site, there are two clades of the family with distinct substrate preference (Fig. 3a). A large and distant branch of the family expressed in prokaryotes has evolved a capability for  $\text{Mg}^{2+}$  transport and was termed NRMT (for NRAMP related  $\text{Mg}^{2+}$  transporters).<sup>[39]</sup> A smaller branch in plants was shown to transport the trivalent ion  $\text{Al}^{3+}$ <sup>[40]</sup> which is found in acid soils and whose accumulation inside cells is toxic owing due to the strong Lewis acidity of the trivalent ion. Both ions are distinguished by their small radius and consequent high surface charge density, which renders them particularly challenging targets for membrane transport. The deviation in the substrate preference from classical SLC11/NRAMP transporters is reflected in the difference in the residues constituting the described metal ion binding site, where the negatively charged aspartate on  $\alpha$ 1 is the only conserved residue of the site, whereas the methionine on  $\alpha$ 6 is replaced by either an alanine or a threonine (Fig. 3a). Since the mere introduction of the NRMT binding site into a classical



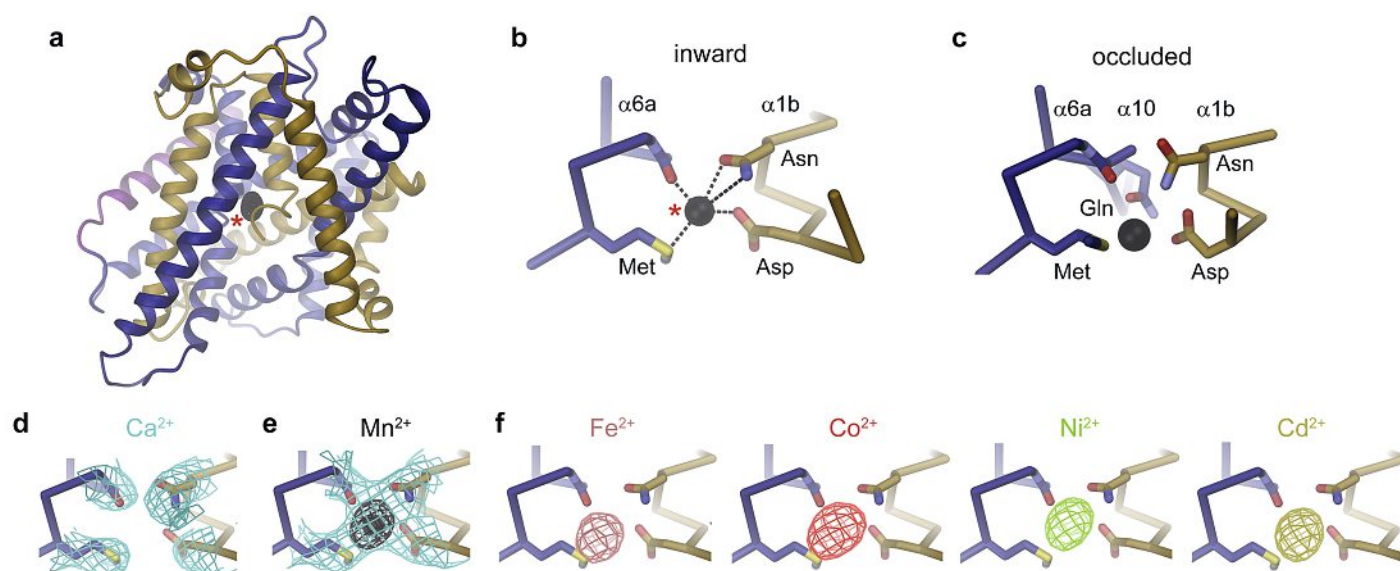


Fig. 2. Transition metal ion binding site. a) Ribbon representation of ScaDMT adopting an inward-facing conformation with anomalous difference density defining the position of a bound  $\text{Mn}^{2+}$  ion (black mesh). b) Blow-up of the ion binding site in the inward-facing conformation of ScaDMT with coordinating interactions indicated by dashed lines. The figure shows conserved residues providing hard ligands (Asp and Asn on  $\alpha 1$  and a back-bone carbonyl on  $\alpha 6$ ) and a Met on  $\alpha 6$  acting as soft ligand for transition metal ion interactions. a,b) Asterisks mark equivalent positions. c) Ion interactions in the occluded conformation of DraNRAMP showing equivalent coordination as in b and an additional interaction with a Gln on  $\alpha 10$ , which has moved towards the ion upon the change of conformations. d) Ion binding region of the protein crystallized in presence of  $\text{Ca}^{2+}$  in absence of transition metal ions shows no ion binding to the site. e) The same region collected from a crystal soaked in  $\text{Mn}^{2+}$  shows ion binding, which is further illustrated in the anomalous difference density (black mesh). d,e) Cyan mesh displays the  $2F_o - F_c$  density of the respective structures. f) Anomalous difference densities (colored mesh) observed in data collected from crystals soaked with indicated metal ions. b–f) The protein is displayed as  $\alpha$ -trace with side-chain and main-chain groups interacting with the ion shown as sticks.

NRAMP transporter was insufficient to confer the capability of  $\text{Mg}^{2+}$  transport,<sup>[38]</sup> it became obvious that properties of the protein beyond the immediate coordinating residues are required to alter the selectivity sufficiently to permit  $\text{Mg}^{2+}$  transport. These requirements were revealed by the characterization of the NRMT from the bacterium *Egerthella lenta* called EleNRMT.<sup>[38]</sup> Whereas this protein is capable of transporting  $\text{Mn}^{2+}$  with micromolar affinity, it also transports  $\text{Mg}^{2+}$  but not  $\text{Ca}^{2+}$ . A study combining data from cryo-electron microscopy (cryo-EM) and X-ray crystallography has defined the basis for the altered selectivity properties.<sup>[38]</sup> This preference is manifested in the structure of the transporter in an inward-facing conformation defined by cryo-EM at high resolution, where the binding of the transported  $\text{Mn}^{2+}$  was demonstrated in complementary X-ray data at lower resolution, exploiting the anomalous scattering properties of the bound substrate (Fig. 3b, c). Although in its general architecture, the protein shows similar overall features with selective transition metal ion transporters of the same family, the volume of the substrate binding site is considerably expanded to permit the binding of a  $\text{Mg}^{2+}$  ion still containing most of its inner hydration shell, thereby avoiding its full dehydration, which would be energetically costly<sup>[38]</sup> (Fig. 3d).

## 7. Proton Coupling

A conserved property of classical SLC11/NRAMP transporters but not of NRMTs concerns the coupling of metal ions to the symport of  $\text{H}^+$  acting as energy source.<sup>[20,25,38]</sup> Whereas a negative membrane potential itself allows a concentration of the positively charged substrate inside the cell (by a factor of  $\sim 170$  for a divalent cation at a membrane potential of  $-70$  mV), the coupled downhill transport of protons along a pH gradient that is established by the acidic environments in the lumen of endosomes and the unstirred layer at the surface of enterocytes, permits a further accumulation of the scarce metal ion. Unlike the defined location of metal ion binding sites,  $\text{H}^+$  can be accepted and released by numerous titratable groups of a protein at appropriate pH values and conducted over larger distances within the protein *via* proton

wires consisting of proximal proton-accepting residues and water molecules. The abundance of such titratable groups complicates the localization of residues involved in  $\text{H}^+$  transport. In case of classical NRAMP transporters,  $\text{H}^+$  transport was associated with two conserved histidine positions located intracellular to the metal ion binding site on  $\alpha$ -helix 6b,<sup>[41]</sup> the metal coordinating aspartate and a chain of charged residues located in a narrow conduit separate from the intracellular ion exit pathway that connects the binding site to the intracellular solution<sup>[25,29,36]</sup> (Fig. 4a). The latter was also proposed based on a study combining computer simulations and electrophysiology performed in the context of the NCCR TransCure.<sup>[42]</sup> Mutations in several residues have compromised coupling thus rendering their involvement in  $\text{H}^+$  transport plausible.<sup>[25,28,43]</sup> Interestingly, the described  $\alpha 6b$  His residues are absent in NRMTs and the charged tunnel observed in the structures of prokaryotic NRAMPs was found to be filled with hydrophobic residues in EleNRMT (Fig. 4b). Together these features coincide with the observed lack of coupled proton transport of EleNRMT<sup>[38]</sup> and thus support the involvement of the described residues in  $\text{H}^+$  conduction.

## 8. Conclusions

The combination of structural and functional approaches has over the last few years provided important insight into the transport mechanisms of SLC11/NRAMP proteins,<sup>[27]</sup> which constitute an important family of transition metal ion transporters that is involved in the uptake of  $\text{Fe}^{2+}$  into the human body and whose regulation was suggested as promising strategy against iron storage diseases.<sup>[44]</sup> These studies revealed how SLC11 transporters efficiently select transition metal ions from a large background of  $\text{Ca}^{2+}$  and  $\text{Mg}^{2+}$  and concentrate these trace elements in the cell by the cotransport of  $\text{H}^+$  serving as energy source. Investigations on the distantly related NRMTs illustrate how the same family has evolved a different selectivity to facilitate the uptake of  $\text{Mg}^{2+}$ , which requires altered binding properties.<sup>[38]</sup> Although past studies have focused on prokaryotic homologs, they now can be

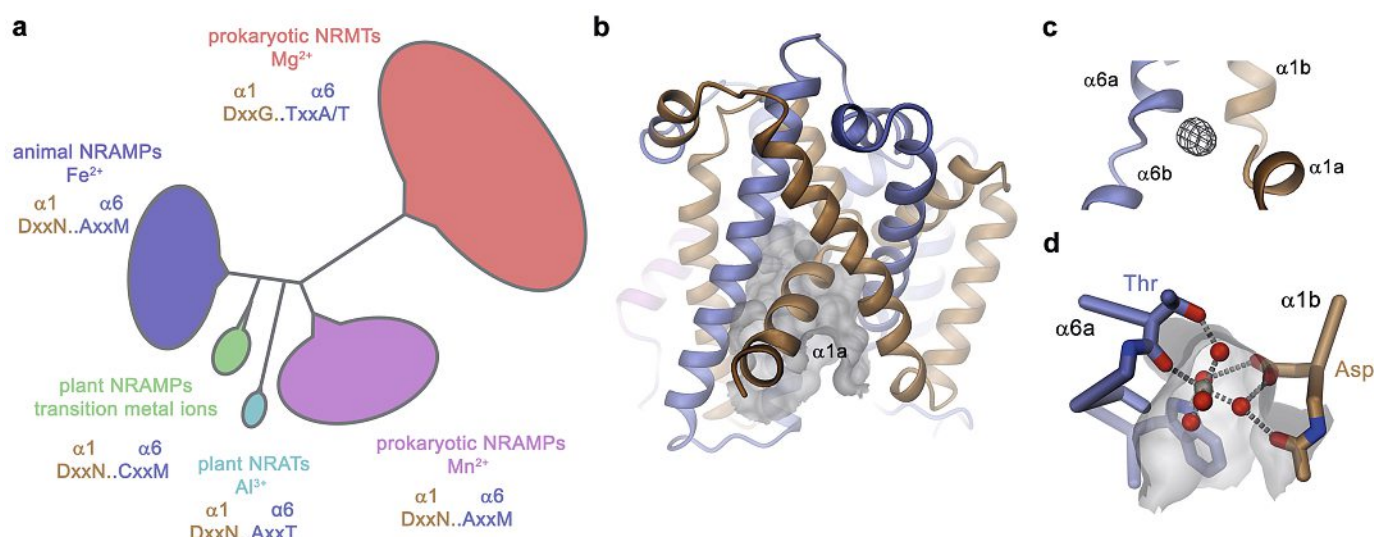


Fig. 3. Structural properties of an NRMT. a) Schematic depiction of the phylogenetic tree of the SLC11 family with different clades indicated as colored balloons and the sequence of the consensus binding site shown. b) Ribbon representation of EleNRMT (PDBID 7QIA) in an inward-facing conformation. c) Ion binding region of EleNRMT with anomalous difference density of bound  $Mn^{2+}$  defining the ion binding site of the protein, which is located in an equivalent position as in ScaDMT. d) Close-up of the ion binding site of EleNRMT interacting with a hydrated  $Mg^{2+}$  ion, whose position was defined by the anomalous density of  $Mn^{2+}$ . The surrounding water molecules are modeled.  $Mg^{2+}$  ions and water molecules are shown as grey and red spheres, respectively. b,d) The molecular surface of the pocket leading to the ion binding site is shown in grey.

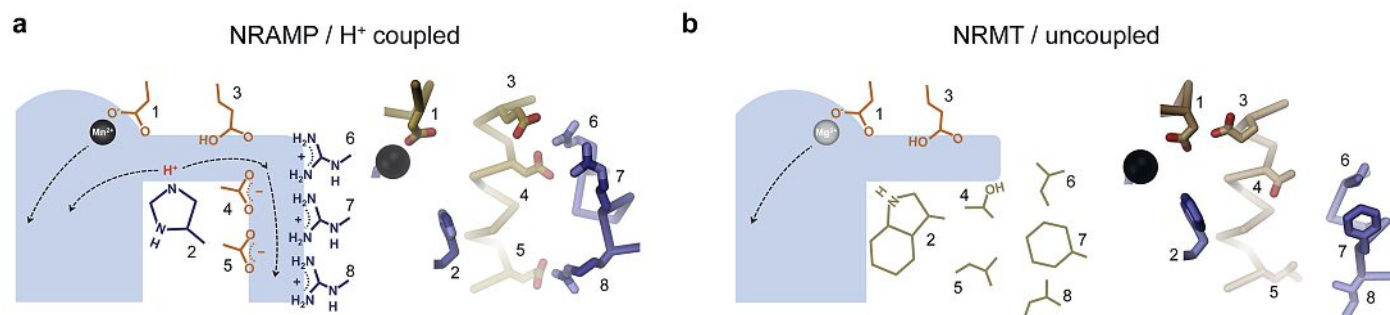


Fig. 4. Putative  $H^+$  coupling mechanism. a) Schematic drawing of a bifurcated putative  $H^+$  release pathway towards the cytoplasm in the inward-facing conformation of coupled transition metal transporters (left) and structure of the equivalent region of ScaDMT (right). b) Corresponding region in an uncoupled NRMT  $Mg^{2+}$  transporter with structural elements of EleNRMT shown on the right. a,b) Equivalent positions are labeled. 2 corresponds to a conserved His in coupled NRAMP transporters that is replaced by a Trp in EleNRMT.

extended towards mammalian family members to characterize the structural and functional differences between the two human SLC11 paralogs and their interaction with accessory proteins that might assist in the transport of these reactive substrates in a cellular environment. The described findings can also be exploited for the development of molecules targeting the transporter to overcome debilitating iron overload disorders.

### Acknowledgements

This work was supported by the Swiss National Science Foundation (SNSF) NCCR TransCure grant # 51NF40-185544 to RD.

Received: September 19, 2022

- [1] E. Carafoli, J. Krebs, *J. Biol. Chem.* **2016**, *291*, 20849, <https://doi.org/10.1074/jbc.R116.735894>.
- [2] J. H. de Baaij, J. G. Hoenderop, R. J. Bindels, *Physiol. Rev.* **2015**, *95*, 1, <https://doi.org/10.1152/physrev.00012.2014>.
- [3] M. E. Maguire, J. A. Cowan, *Biometals* **2002**, *15*, 203, <https://doi.org/10.1023/a:1016058229972>.
- [4] R. Williams, *Royal Institute of Chemistry, Reviews* **1968**, *1*, 13, <https://doi.org/10.1039/RR9680100013>.
- [5] D. H. Nies, G. Grass, *EcoSal Plus* **2009**, *3*, <https://doi.org/10.1128/ecosalplus.5.4.4.3>.
- [6] M. M. Harding, *Acta Crystallogr. D Biol. Crystallogr.* **2004**, *60*, 849, <https://doi.org/10.1107/S0907444904004081>.
- [7] L. Rulisek, J. Vondrasek, *J. Inorg. Biochem.* **1998**, *71*, 115, [https://doi.org/10.1016/s0162-0134\(98\)10042-9](https://doi.org/10.1016/s0162-0134(98)10042-9).
- [8] D. A. Gell, *Blood Cells Mol. Dis.* **2018**, *70*, 13, <https://doi.org/10.1016/j.bcmd.2017.10.006>.
- [9] Y. M. Xiu, *Biomed. Environ. Sci.* **1996**, *9*, 130.
- [10] N. Montalbetti, A. Simonin, G. Kovacs, M. A. Hediger, *Mol. Aspects Med.* **2013**, *34*, 270, <https://doi.org/10.1016/j.mam.2013.01.002>.
- [11] A. Rolfs, H. L. Bonkovsky, J. G. Kohlroser, K. McNeal, A. Sharma, U. V. Berger, M. A. Hediger, *Am. J. Physiol. Gastrointest. Liver Physiol.* **2002**, *282*, G598, <https://doi.org/10.1152/ajpgi.00371.2001>.
- [12] H. Gunshin, B. Mackenzie, U. V. Berger, Y. Gunshin, M. F. Romero, W. F. Boron, S. Nussberger, J. L. Gollan, M. A. Hediger, *Nature* **1997**, *388*, 482, <https://doi.org/10.1038/41343>.
- [13] Y. Nevo, N. Nelson, *Biochim. Biophys. Acta* **2006**, *1763*, 609, <https://doi.org/10.1016/j.bbamer.2006.05.007>.
- [14] S. M. Vidal, D. Malo, K. Vogan, E. Skamene, P. Gros, *Cell* **1993**, *73*, 469, [https://doi.org/10.1016/0092-8674\(93\)90135-d](https://doi.org/10.1016/0092-8674(93)90135-d).
- [15] S. Tandy, M. Williams, A. Leggett, M. Lopez-Jimenez, M. Dedes, B. Ramesh, S. K. Srari, P. Sharp, *J. Biol. Chem.* **2000**, *275*, 1023, <https://doi.org/10.1074/jbc.275.2.1023>.
- [16] H. Makui, E. Roig, S. T. Cole, J. D. Helmann, P. Gros, M. F. Cellier, *Mol. Microbiol.* **2000**, *35*, 1065, <https://doi.org/10.1046/j.1365-2958.2000.01774.x>.
- [17] M. F. Cellier, I. Bergevin, E. Boyer, E. Richer, *Trends Genet.* **2001**, *17*, 365, [https://doi.org/10.1016/s0168-9525\(01\)02364-2](https://doi.org/10.1016/s0168-9525(01)02364-2).

- [18] X. Huang, S. Duan, Q. Wu, M. Yu, S. Shabala, *Plants (Basel)* **2020**, *9*, <https://doi.org/10.3390/plants9020223>.
- [19] A. C. Illing, A. Shawki, C. L. Cunningham, B. Mackenzie, *J. Biol. Chem.* **2012**, *287*, 30485, <https://doi.org/10.1074/jbc.M112.364208>.
- [20] B. Mackenzie, M. L. Ujwal, M. H. Chang, M. F. Romero, M. A. Hediger, *Pflügers Arch.* **2006**, *451*, 544, <https://doi.org/10.1007/s00424-005-1494-3>.
- [21] B. Mackenzie, H. Takanaga, N. Hubert, A. Rolfs, M. A. Hediger, *Biochem. J.* **2007**, *403*, 59, <https://doi.org/10.1042/BJ20061290>.
- [22] A. Shawki, B. Mackenzie, *Biochem. Biophys. Res. Commun.* **2010**, *393*, 471, <https://doi.org/10.1016/j.bbrc.2010.02.025>.
- [23] I. A. Ehrnstorfer, E. R. Geertsma, E. Pardon, J. Steyaert, R. Dutzler, *Nat. Struct. Mol. Biol.* **2014**, *21*, 990, <https://doi.org/10.1038/nsmb.2904>.
- [24] A. T. Bozzi, L. B. Bane, W. A. Weihofen, A. L. McCabe, A. Singharoy, C. J. Chipot, K. Schulten, R. Gaudet, *Proc. Natl. Acad. Sci. U S A* **2016**, *113*, 10310, <https://doi.org/10.1073/pnas.1607734113>.
- [25] I. A. Ehrnstorfer, C. Manatschal, F. M. Arnold, J. Laederach, R. Dutzler, *Nat. Commun.* **2017**, *8*, 14033, <https://doi.org/10.1038/ncomms14033>.
- [26] C. Manatschal, J. Pujol-Gimenez, M. Poirier, J. L. Reymond, M. A. Hediger, R. Dutzler, *eLife* **2019**, *8*, <https://doi.org/10.7554/eLife.51913>.
- [27] A. T. Bozzi, R. Gaudet, *J. Mol. Biol.* **2021**, *433*, 166991, <https://doi.org/10.1016/j.jmb.2021.166991>.
- [28] A. T. Bozzi, L. B. Bane, W. A. Weihofen, A. Singharoy, E. R. Guillen, H. L. Ploegh, K. Schulten, R. Gaudet, *Structure* **2016**, *24*, 2102, <https://doi.org/10.1016/j.str.2016.09.017>.
- [29] A. T. Bozzi, L. B. Bane, C. M. Zimanyi, R. Gaudet, *J. Gen. Physiol.* **2019**, *151*, 1413, <https://doi.org/10.1085/jgp.201912428>.
- [30] A. Yamashita, S. K. Singh, T. Kawate, Y. Jin, E. Gouaux, *Nature* **2005**, *437*, 215, <https://doi.org/10.1038/nature03978>.
- [31] J. A. Coleman, E. M. Green, E. Gouaux, *Nature* **2016**, *532*, 334, <https://doi.org/10.1038/nature17629>.
- [32] S. Faham, A. Watanabe, G. M. Besserer, D. Cascio, A. Specht, B. A. Hirayama, E. M. Wright, J. Abramson, *Science* **2008**, *321*, 810, <https://doi.org/10.1126/science.1160406>.
- [33] S. Ressler, A. C. Terwisscha van Scheltinga, C. Vornrhein, V. Ott, C. Ziegler, *Nature* **2009**, *458*, 47, <https://doi.org/10.1038/nature07819>.
- [34] T. A. Chew, B. J. Orlando, J. Zhang, N. R. Latorraca, A. Wang, S. A. Hollingsworth, D. H. Chen, R. O. Dror, M. Liao, L. Feng, *Nature* **2019**, *572*, 488, <https://doi.org/10.1038/s41586-019-1438-2>.
- [35] O. Jardetzky, *Nature* **1966**, *211*, 969, <https://doi.org/10.1038/211969a0>.
- [36] A. T. Bozzi, C. M. Zimanyi, J. M. Nicoludis, B. K. Lee, C. H. Zhang, R. Gaudet, *eLife* **2019**, *8*, <https://doi.org/10.7554/eLife.41124>.
- [37] D. Drew, O. Boudker, *Annu. Rev. Biochem.* **2016**, *85*, 543, <https://doi.org/10.1146/annurev-biochem-060815-014520>.
- [38] K. Ramanadane, M. S. Straub, R. Dutzler, C. Manatschal, *eLife* **2022**, *11*, <https://doi.org/10.7554/eLife.74589>.
- [39] J. H. Shin, C. A. Wakeman, J. R. Goodson, D. A. Rodionov, B. G. Freedman, R. S. Senger, W. C. Winkler, *PLoS Genet.* **2014**, *10*, e1004429, <https://doi.org/10.1371/journal.pgen.1004429>.
- [40] J. Xia, N. Yamaji, T. Kasai, J. F. Ma, *Proc. Natl. Acad. Sci. U S A* **2010**, *107*, 18381, <https://doi.org/10.1073/pnas.1004949107>.
- [41] S. Lam-Yuk-Tseung, G. Govoni, J. Forbes, P. Gros, *Blood* **2003**, *101*, 3699, <https://doi.org/10.1182/blood-2002-07-2108>.
- [42] J. Pujol-Gimenez, M. A. Hediger, G. Gyimesi, *Sci. Rep.* **2017**, *7*, 6194, <https://doi.org/10.1038/s41598-017-06446-y>.
- [43] A. T. Bozzi, A. L. McCabe, B. C. Barnett, R. Gaudet, *J. Biol. Chem.* **2020**, *295*, 1212, <https://doi.org/10.1074/jbc.RA119.011336>.
- [44] B. J. Crielgaard, T. Lammers, S. Rivella, *Nat. Rev. Drug Discov.* **2017**, *16*, 400, <https://doi.org/10.1038/nrd.2016.248>.

#### License and Terms



This is an Open Access article under the terms of the Creative Commons Attribution License CC BY 4.0. The material may not be used for commercial purposes.

The license is subject to the CHIMIA terms and conditions: (<https://chimia.ch/chimia/about>).

The definitive version of this article is the electronic one that can be found at <https://doi.org/10.2533/chimia.2022.1005>